

Integrated source of telecom-band photon-pairs based on high index silica glass spiral waveguides

Liang Cui,¹ Hao Feng,¹ Xiaotian Zhu,² Changyue Wang,¹ Z. Y. Ou,^{2†} Xiaoying Li,^{1*} Brent E. Little,³ and Sai T. Chu²

¹ College of Precision Instrument and Opto-Electronics Engineering, Key Laboratory of Opto-Electronics Information Technology, Ministry of Education, Tianjin University, Tianjin 300072, China

² Department of Physics, City University of Hong Kong, 83 Tat Chee Avenue, Kowloon, Hong Kong, China

³ QXP Inc., Xi'an, China

*xiaoyingli@tju.edu.cn, †jeffou@cityu.edu.hk

Abstract: We generate correlated photon-pairs via spontaneous four-wave mixing in high index silica glass spiral waveguides. Results show that spontaneous Raman scattering is the main noise origin, and propagation loss limits the optimum length of waveguides. © 2022 The Author(s)

1. Introduction

Quantum light sources such as single-photon sources and entangled photon-pair sources play a key role in discrete-variable quantum information processing (QIP). Compact, flexible, and low energy consumption devices are highly desirable in QIP applications. Therefore, recent years have witnessed the rapid development of on-chip quantum light sources based on integrated nonlinear waveguides [1].

The high index doped silica glass (HDSG, $n=1.7$) is one of the promising platforms for developing integrated optical devices [2]. The mature technology allows fabrication of micro-ring resonators or spiral waveguides with length of more than one meter. These HDSG devices are suitable for nonlinear optics applications due to the properties of low-loss and relatively higher nonlinearity. Multiphoton entangled state have been created by using the frequency comb based on spontaneous four-wave mixing (FWM) in HDSG micro-ring resonators [3]. Optical parametric amplification also have been demonstrated via stimulated FWM in the HDSG spiral waveguides [4].

In this paper, we utilize the spontaneous FWM in HDSG spiral waveguides to generate quantum correlated photon-pairs. The photon-pairs are created via a one-pass process and have a broadband nature, which is different from the case of using a micro-ring resonator. We also examine the influences of spontaneous Raman scattering and the propagation loss in the waveguides.

2. Experimental results

2.1. Setup

The two HDSG spiral waveguides used in our experiment have the same rectangular cross section with a size of $1.25 \mu\text{m} \times 4 \mu\text{m}$ (thickness \times width), while the lengths of the two waveguides are 0.5 m and 1 m, respectively. As shown in Fig. 1(a), the spiral waveguides are contained in an area less than $0.5 \text{ cm} \times 0.5 \text{ cm}$, and their input/output ports are coupled to standard single-mode fibers (SMF). The coupling loss is $\sim 0.4 \text{ dB/facet}$. The propagation loss in the waveguides is $\sim 0.08 \text{ dB/cm}$ (@1550 nm). The group velocity dispersion of the TE mode is around 10 ps/km/nm in the 1550 nm band, which is suitable for FWM process with a gain bandwidth of tens of nanometers.

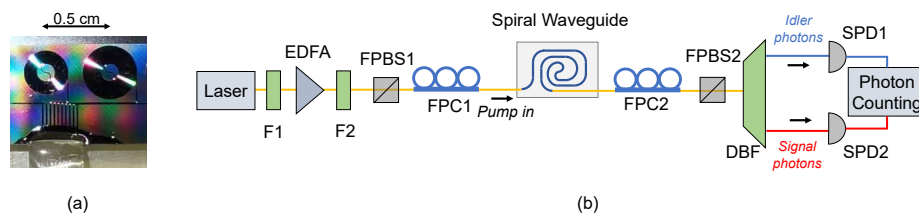


Fig. 1. (a) Two HDSG spiral waveguides on a chip. (b) Experimental setup. F, Filter; FPBS, Fiber polarization beam splitter; FPC, Fiber polarization controller; DBF, Dual band filter; SPD, Single photon detector.

Based on the dispersion property, we build the experimental setup shown in Fig. 1(b) to observe the photon-pair generation. The pump source is a telecom band mode-locked fiber laser with a repetition rate of 36.9 MHz. We carve out and amplify the pump by using two bandpass filters (F1 and F2) and an Erbium-doped fiber amplifier (EDFA). The central wavelength of the pump launched into the waveguide is 1554.94 nm. By changing F1 and F2, the full width at half-maximum (FWHM) of the pump $\Delta\lambda_p$ can be adjusted. In front of the waveguide, we employ a fiber polarization beam splitter (FPBS1) to purify the polarization state of the pump, and a fiber polarization controller (FPC1) to ensure that the TE mode is exited.

At the output port of the waveguide, we employ another set of FPC2 and FPBS2 to select the TE mode light. Then we use a dual band filter (DBF) to respectively collect the signal and idler correlated photons and block the residual pump. The DBF consists of a notch filter and a two-channel bandpass filter, and has an isolation of about 120 dB to the pump. Since the gain bandwidth of FWM is broad, we set the central wavelengths of the two channels for the signal and idler photons to 1561.42 nm and 1548.51 nm, respectively, and the FWHM of both channels is restricted to 1.5 nm. We use two superconducting nanowire single photon detectors (SPDs) to detect the signal and idler photons and a computer-based photon counting system to proceed the data. The total efficiency of filtering and detection for the signal and idler photons is about 12%.

2.2. Photon-pair generation and influence of Raman scattering

We first observe the photon-pair generation in the 0.5-m-long spiral waveguide. In the experiment, we adjust the pump power and record the single-channel photon counting rate measured by the two SPDs as well as the coincidence counting rate between them. The left and central columns in Fig. 2 show the results when the FWHM of pump $\Delta\lambda_p$ is 0.35 nm and $\Delta\lambda_p=0.7$ nm, respectively.

The data points in Figs. 2(a) and 2(b) are the measured single-channel counting rates of the idler photons as a function of the average pump power P_a . Generally, the production rates of FWM photons and Raman photons are proportional to $P_p^2 L^2 \Delta t$ and $P_p L \Delta t$, respectively, where L is the length of the waveguide, P_p and Δt are the peak power and pulse duration of the pulsed pump [5]. The peak power and average power are related via $P_p = P_a / \Delta t$. Based on the different dependence of the FWM and Raman photons on the average pump power, we fit the two sets of data by using polynomial $xP_a + yP_a^2$ (the solid lines), where the quadratic term yP_a^2 (the dashed lines) and linear term xP_a (the dotted lines) respectively represent the amounts of photons originate from FWM and Raman scattering. The fitting results indicate that there is a significant number of photons from Raman scattering. Since the Raman photons from the SMF pigtailed are negligible, the waveguide is the only origin of these Raman photons.

Figures 2(d) and 2(e) show the measured coincidence counting rates and the coincidence to accidental-coincidence ratio (CAR). When the coincidence rate is 0.9 kHz, the CAR is about 33, which clearly shows the quantum correlation between the signal and idler photons. Due to the multi-photon events, the CAR declines with the increase of the coincidence rates .

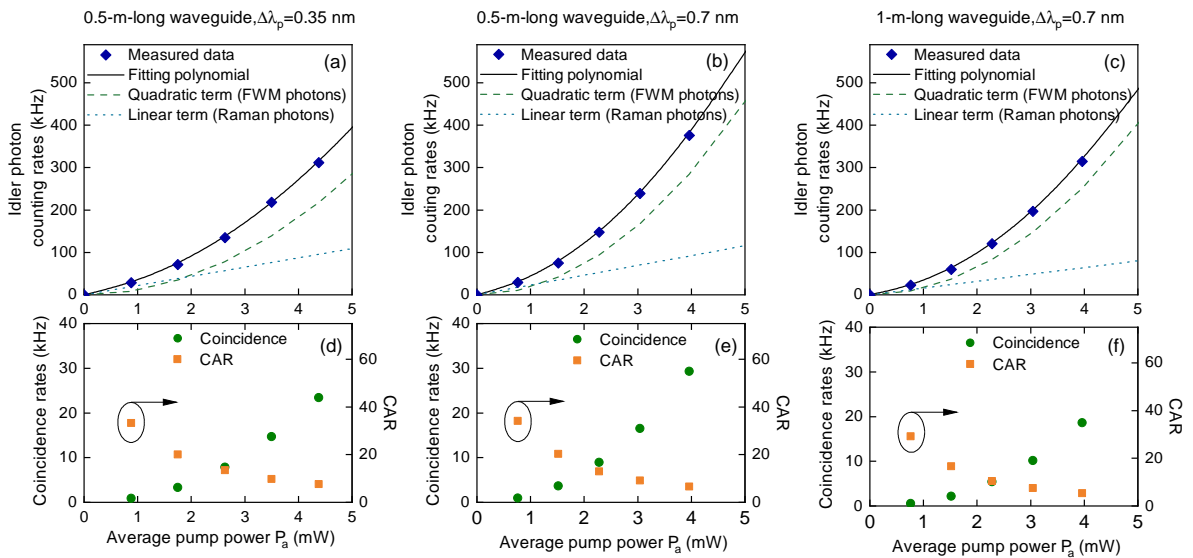


Fig. 2. (a)-(c): Single-channel counting rates of the idler photons as a function of average pump power P_a . The data points is fitted by a quadratic polynomial (solid lines), where the quadratic term (dashed lines) and linear term (dotted lines) represent photons from FWM and Raman scattering, respectively. (d)-(f): Measured coincidence counting rates and CAR versus P_a .

Comparing the results of $\Delta\lambda_p=0.35$ nm and $\Delta\lambda_p=0.7$ nm, one sees that, at the same average pump power, the number of FWM photons in the latter case is higher than that in the former case, but the number of Raman photons is almost the same in both cases. This can be explained by the different dependence of FWM and Raman photons on the peak pump power: using a pump with a larger bandwidth (shorter pulse duration) can increase the portion of FWM photons.

2.3. Influence of propagation loss in the waveguide

To show the influence of the propagation loss, we replace the 0.5-m-long waveguide with the 1-m-long waveguide and repeat the measurement. The results for $\Delta\lambda_p=0.7$ nm are shown in Figs. 2(c) and 2(f). According to the previous discussion, the production rate of FWM photons should be proportional to the square of waveguide length L^2 . However, comparing the results in Figs. 2(b) and 3(c), one sees that the total photon counting rates of the 1-m-long waveguide is even lower than that of the 0.5-m-long waveguide. Furthermore, we plot the coincidence rate as a function of the counting rate of FWM photons for both cases, as shown in Fig. 3. The results indicate that the photon-pair collection efficiency is lower for the 1-m-long waveguide case. This is because the photons experience higher propagation loss in the 1-m-long waveguide, so more correlated photons lose their counterparts. Generally, considering the propagation loss in the waveguide, using a longer waveguide may not be an optimum choice.

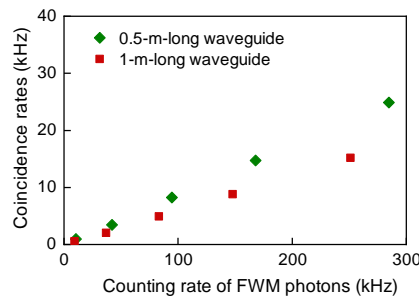


Fig. 3. Measured coincidence counting rate as a function of the counting rate of FWM photons.

3. Conclusion

We demonstrate the generation of quantum correlated photon-pairs via spontaneous FWM in two 0.5- and 1-m-long HDSG spiral waveguides. Besides the quantum correlation between the signal and idler photons, results also show that the spontaneous Raman scattering is still a main noise origin. Moreover, considering the propagation loss in the waveguides, an optimum length of waveguide should be carefully determined.

Further experiments, including cooling the waveguide chip to suppress the Raman scattering photons and spectral measurement of the photon-pairs, are undergoing. More results will be presented on the conference.

References

1. G. Moody, L. Chang, T. J. Steiner, and J. E. Bowers, “Chip-scale nonlinear photonics for quantum light generation,” *AVS Quantum Sci.* **2**, 041702 (2020).
2. D. J. Moss, A. Pasquazi, M. Peccianti, L. Razzari, D. Duchesne, M. Ferrera, S. Chu, B. E. Little, and R. Morandotti, “CMOS compatible waveguides for all-optical signal processing,” in *Proc.SPIE*, vol. 7942 (2011), p. 794205.
3. C. Reimer, M. Kues, P. Roztocky, B. Wetzel, F. Grazioso, B. E. Little, S. T. Chu, T. Johnston, Y. Bromberg, L. Caspani, D. J. Moss, and R. Morandotti, “Generation of multiphoton entangled quantum states by means of integrated frequency combs,” *Science* **351**, 1176–1180 (2016).
4. A. Pasquazi, Y. Park, J. Azaña, F. Légaré, R. Morandotti, B. E. Little, S. T. Chu, and D. J. Moss, “Efficient wavelength conversion and net parametric gain via four wave mixing in a high index doped silica waveguide,” *Opt. Express* **18**, 7634–7641 (2010).
5. L. Cui, X. Li, C. Guo, Y. H. Li, Z. Y. Xu, L. J. Wang, and W. Fang, “Generation of correlated photon pairs in micro/nano-fibers,” *Opt. Lett.* **38**, 5063–5066 (2013).